

DEPARTMENT OF METALLURGY AND MATERIALS SCIENCE

TIME - OF - FLIGHT DETECTION OF GALLIUM CLUSTER - IONS

UNIVERSITY OF CAMBRIDGE

TIME-OF-FLIGHT DETECTION OF GALLIUM CLUSTER-IONS

A.R. Waugh

This report is a summary of work carried out in the Department of Metallurgy and Materials Science, University of Cambridge, between October 1978 and October 1979, under Culham EMR Contract Cul/22.

Introduction

It was agreed at a meeting between Culham and Cambridge that a suitable starting point for this project would be the construction of a time-of-flight mass-spectrometer: this was to be used to characterize liquid-metal ion sources of Culham design, with a particular emphasis on determining the proportion and mass-to-charge ratio of any metal cluster-ions, or charged droplets, in the eflux from the sources. A time-of-flight spectrometer was chosen, rather than a quadrupole or a magnetic spectrometer, as being easier to construct to detect very heavy ion clusters, and because of the high sensitivity which is attainable with such instruments.

This report describes the spectrometer which has been constructed and gives results obtained from a Culham-supplied gallium-ion source. Significant proportions of Ga_n^+ cluster ions have been detected, for $1 \leq n \leq 7$. It is suggested that the origin of such clusters can best be determined by measurements of the energy-distributions of the clusters.

Data is also presented which shows the effects of raising the source voltage with 10 nS and 70 μ S high-voltage pulses. It is shown that nanosecond pulsing leads to a widening of the energy-distribution of the ions, while microsecond pulsing can lead to a useful modulation of the beam current; operation of the source only for the duration of the pulses proved to be possible.

Time-of-flight Mass Spectrometry

The time-of-flight (TOF) mass spectrometer is simple in conception when compared to magnetic or quadrupole spectrometers. Ions from the beam to be mass-analyzed are only allowed to enter a drift-tube during a short time-interval; provided that the ions have the same energy ($E = neV$, where V is the ion accelerating potential) then a measurement of the time interval between the ions entering the tube and an ion arriving at a detector at the far end gives its mass-to-charge ratio, since the velocity $v = L/t$ (t is the flight time over distance L) and $\frac{1}{2} m v^2 = neV$, so $m/ne = 2V/v^2 = 2Vt^2/L^2$. The 'chopping' of the ion beam, to determine the start time, can be accomplished with a retarding grid (suitable for low-energy ions) or by sweeping the beam across an aperture (suitable for higher-energy ions, as in the work reported here).

The apparatus constructed to analyse the ion-beam from the liquid-metal sources is shown in figure 1. The source (1) is mounted so that it can be tilted about its exit aperture, to allow the investigation of the beam profile, and can be moved bodily to allow alignment with the spectrometer apertures. A collector (2) with a small central aperture allows the measurement of the overall ion current. A razor-edged slit (3) behind the aperture in (2) defines the beam to be analyzed. A slit lens (4) focusses the beam to be roughly parallel. It then enters the deflection field between two short parallel plates, one of which is grounded (5) and one of which (6) can be biased positive, to deflect the beam, and ^{then} pulsed down to zero, to allow the beam to sweep across the second razor-edged slit (7). The ion-pulse thus selected can be deflected by X and Y plates (8 and 9) so that the ions reach the detector, a Bendix M 300 electron multiplier (10), at the other end of the 75 cm drift tube. Intermediate apertures (11 and 12) are to prevent scattered ions reaching the detector. A bellows (13) allows the whole ion-source and deflection system to be tilted, so that neutrals or photons are prevented from reaching the

detector by the apertures, while the ions can be deflected by the plates (9) onto the detector.

The chopping pulse is generated by the circuit in figure 2. A variable-length 5 volt pulse ($100 \mu\text{S} - 2 \text{ mS}$) is fed to the base of one of two transistors (T1, T2) operating in avalanche mode: these fire on the leading edge of the pulse, rapidly discharging a capacitor C and generating a negative-going sweep voltage of $\sim 10 \text{ nS}$ fall-time and 300 V amplitude. Charging of the capacitor C is controlled by charging resistors R and by a clamping high-voltage transistor T3 which prevents recharging until the end of the trigger pulse; this ensures that the beam, after being swept across the slit (7), remains off it until the longest flight-time of interest has occurred. Charging then recommences and the cycle can be repeated at $\sim 5 \text{ KHz}$ (depending on the hold-off time).

The output from the electron multiplier can be switched to one or other of two amplifiers. One uses a SN72733 integrated circuit (figure 3) connected as a broadband (100 MHz) linear amplifier with a gain of 10. The output from this is monitored on a fast oscilloscope (100 MHz bandwidth). Alternatively, a non-linear amplifier is used which emits a TTL logic pulse whenever the multiplier current exceeds a threshold: this is sensitive enough to be triggered by the multiplier current which results from the arrival of individual ions.

Display of the mass spectrum

The mass spectrum can be recorded in one of three ways:-

- a) By photographing the linearly-amplified multiplier current, displayed as vertical amplitude on a linearly-swept oscilloscope trace
- b) By photographing the pulse output from the non-linear amplifier, similarly displayed on the oscilloscope.

or c) by using the spectrometer sweep pulse to start a digital timer: the arrival times of successive ions are then recorded by a small computer, and a histogram showing the number of ions of a given flight time is built up by repeatedly pulsing the spectrometer.

Method a) is useful in giving an immediate indication of the overall mass spectrum (figure 4). However, it is difficult to obtain sufficient resolution from a CRO trace to observe the weakest peaks in the spectrum as well as high-intensity peaks; it is also difficult to integrate successive sweeps unless a very fast transient digitiser is available.

Method b) is a convenient, but non-quantitative, way of determining the presence or absence of small numbers of ions of a given mass in the beam: if some thousands of successive sweeps are recorded one frame of film, with a suitable camera aperture, then noise signals at random times in the sweep will produce a faint background blur, while signals at specific times due to genuine ions will reinforce, so that the photograph has a series of vertical lines at the flight-times of genuine ions (figure 5).

Method c) has potential advantages in quantifying the number of rare ions (e.g. heavy clusters) present, since these can be counted individually, and, with a sufficiently long integration time, distinguished from any noise present. If the histogram of flight-times is to be quantitative it is important that the ion current should be low, so that there is a negligible probability of two ions arriving at the detector at the same time, as they would then be recorded as one ion only. The timing system should also be capable of recording several ions arriving at different times in the same sweep. The timer used at present is a 2-channel device with ± 10 nS resolution, developed originally for atom-probe field-ion microscopy. The ion-current from the gallium source was sufficiently intense for there to be a high probability

of more than one Ga^+ , Ga_2^+ or Ga_3^+ ion to arrive at the detector on any one sweep. In order to allow the rarer Ga_4^+ , Ga_5^+ , etc. ions to be observed, without the two available timer channels being taken by Ga^+ and Ga_2^+ ions, the detector output pulses were inhibited during an adjustable delay-time after the start-time, so that the late ions would be the ones to stop the timer. The overall system, which includes a KIM-1 microprocessor to record the flight-times on punched tape for subsequent analysis and histogram-plotting using the University Computer Service IBM 370, is shown in figure 6. A specimen mass spectrum, with Ga^+ and Ga_2^+ largely suppressed for the reasons discussed above, is shown in figure 7. It is seen that peaks due to Ga^+ , Ga_2^+ , Ga_3^+ , Ga_4^+ , Ga_5^+ , Ga_6^+ and possible Ga_7^+ are present in the spectrum: the heavier clusters (Ga_5^+ onwards) recorded here have not apparently been observed previously by other workers using less-sensitive techniques. The heavy clusters are also recorded in figure 5, shown above; Ga^{++} is also commonly observed.

Discussion of results

The relative abundances of the complexes Ga_n^+ were estimated, by counting the number of ions in each peak in the histogram (figure 7) for $n \gg 3$, and by determining the relative abundances of Ga^{++} , Ga^+ , Ga_2^+ and Ga_3^+ from the peak heights in the output from the linear amplifier (figure 4); this last measurement is difficult to do with accuracy. The approximate relative abundances of the ions were:-

Ga^{++}	Ga^+	Ga_2^+	Ga_3^+	Ga_4^+	Ga_5^+	Ga_6^+	Ga_7^+
.5	: 100	: 5-10	: 2-4	: .56	: .19	: .13	: .06

(Ga_3^+ was taken as 3 for Ga_{4-7}^+).

There does not appear to be any specially large abundance for Ga_7^+ , although the literature suggests that M_7^+ is often more common than Ga_6^+ and Ga_5^+ in clusters from ion-bombardment of solids, from arcs in metal vapours, and from gaseous after-glows.

It is interesting to compare the present data with those of Sudreau and coworkers for Au_n^+ :-

Au	Au^+	Au_2^+	Au_3^+	Au_4^+	Au_5^+	Au_6^+	Au_7^+
	100	: 15	: 7	: .9	: .8	: .15	: .15

(taken from a graph in their paper)

In both cases an approximately exponential relationship between the number N_n of ions containing n atoms is observed:-

$$N_n = N_1 \exp(-nK), \text{ where } K \approx 1.15 \text{ for Ga and } 1 \text{ for gold.}$$

Such a distribution could arise for a number of different reasons - e.g. a thermal distribution, with the n^{th} energy level a distance $n\epsilon$ above the ground state, with $N_n = N_1 \exp(-n\epsilon/kT)$: this would give $\epsilon \approx .005$ eV at $T = 300$ K, or $\epsilon \approx .022$ eV at $T = 1400$ K, for gallium. Such energy levels might perhaps correspond to dipole-dipole interactions of polarized neutral atoms (if the electric field and polarizability were high enough) leading to a distribution of neutral clusters in the vapour around the emitter: an equal probability of ionization of the clusters would preserve this distribution for the resulting ions. Evidently, further

information is needed to discriminate between such a model and other models (e.g. involving ion-neutral collisions) which might produce a similar distribution of clusters. The most promising source of further information appears to be measurements on the energy-distributions of the various clusters, since these distributions can suggest both the place of origin of the ions relative to the emitter surface (Sudreau et al. 1979) and also the probability of collisions subsequent to ion formation (Dixon 1979).

It seems clear that there is need for considerably more work, both in collecting experimental data from systems other than gallium and gold, and in theoretical calculations, before the mechanism of source operation is understood. The most complete theoretical modelling so far appears to be that of Gomer (1979). He calculates that

- 1) the source is space-charge limited, leading to 'quiet' current flow
- 2) the source tip is warmed considerably by electron impact and other effects
- 3) field-desorption (ionization directly from the liquid surface) cannot account for the observed currents, which must therefore come from vapour-phase ionization
- 4) ion-impact ionization will not account for the primary current
- 5) electron-impact ionization will contribute at very high currents, producing ions with a large energy spread, but again will not account for the primary current.

As a result of these calculations Gomer suggests that field-ionization of gallium vapour is responsible for the observed currents, with ion-impact producing the observed photon emission and some of the energy-spread of the ions; Dixon (1979) also concludes that the secondary peaks in Sudreau's gold-ion spectra are due to ion-neutral collisions. However, field-ionization requires a field $\geq 5 \times 10^7$ V/cm for the rate of ionization to lead to observable currents; this implies that the tip of the emitter has a radius less than 40 Å. This is much smaller than

has been suggested by electron microscopy ($\sim 1\mu\text{m}$) and it is doubtful whether such a sharp liquid cone would be stable under the extremes of field, temperature, electron bombardment and mass-transport which appear to be necessary. It is conceivable that ionization might result from field-ionization of vapour above small, transient, 'micro-tips' formed on the apex of the observed blunter Taylor cone: direct observation of the ion emission pattern using an imaging system might give a clue to this, especially if sub-microsecond exposures could be obtained to view transient phenomena; such experiments should be possible using channel-plate image intensification.

The effects of externally-applied pulses on the Ga emitter

The effect of increasing the ion-source high-voltage supply by applying 15 nS and 70 μ S high-voltage pulses was investigated. This had two purposes. Firstly, it is known from experiments on the field-ionization of solid field-ion emitters that the charge of the emitted ions can be a sensitive function of field: the possibility therefore arises that the abundance of, for example, Ga^{++} in the beam might be increased by rapidly raising the electric field at the emitter surface. The second reason was to investigate whether the beam intensity could be readily modulated; this might prove very useful in ion-beam lithography, for example.

To investigate the effect of field on charge states it was felt desirable to use the shortest possible pulse, to discourage alterations in the emitting area geometry. Pulses with a short rise-time and an approximately exponentially-decreasing tail were generated by discharging a capacitor with a mercury-wetted reed relay as switch; the pulse amplitude could be varied between 500 V and 2700 V, and the pulse rise-time was < 1 nS, with a pulse length to $\frac{1}{2}$ -maximum of ~ 10 nS.

It was found, perhaps surprisingly, that the 10 nS pulses did not significantly alter the amount of Ga^{++} in the beam, and had only a small effect on the current flowing. Instead, the main effect of the pulses was to greatly broaden the spread of energy of ions in the beam. This was shown by synchronising the pulse applied to the emitter with the sweep pulse of the spectrometer, with a delay between them adjusted to allow time for the ions produced during the pulse to travel to the position of the sweep electrodes; this required a delay of ~ 500 nS (depending on which ion species was being investigated) stable to ~ 1 nS. A sequence of photographs of the spectrometer output as the delay was varied are shown in figure 8. It is seen that the low-energy peak, due to ions formed before the pulse, has been joined by a signal

37
at a shorter flight-time due to Ga^+ ions of higher energy formed during the pulse. Progressively shortening the delay allows ions of progressively higher energy to be observed, up to a cut-off point where the ions have an extra energy corresponding to acceleration by the peak voltage of the pulse. For a pulse amplitude of 1.9 kV the energy increased at the cut-off, measured from the decrease in flight-time, was 1.8 keV, in good agreement. Similar results were observed for Ga^{++} when the delay was adjusted for the longer flight-time of the heavier ion.

The difference between this behaviour and that of a solid emitter at low temperatures should be noted. For the solid emitter the field-evaporation rate is a sensitive function of field. For a typical situation in field-ion microscopy a 10 ns pulse would be used to remove no more than 1 atomic layer of the surface, so that little blunting of the emitter occurs and the sole effect of the pulse is to produce a rapid increase in field and hence evaporation rate. The result is that the ions are formed predominantly during the peak of the pulse and have a relatively small spread in energy. For example, the effect of 3 kV pulses applied to tungsten emitters at 78 K was to produce an energy spread of only 500 volts in the energy of W^+ ions (Krishnaswamy and Muller 1974)

For liquid emitters the high current means that blunting of the emitter can be rapid. A total current of 100 μA corresponds to 1.2×10^{-8} c.c. of gallium per second, or 12×10^{-18} c.c./ns. The emitter tip radius must certainly be less than a few microns, and may be as small as a few nanometres. Evidently, if the flow of gallium into the tip cannot respond rapidly to the increased current during a pulse, then any attempt to increase the current with a pulse even of nanosecond risetime will merely blunt the emitter, and the field at the tip will be little altered. A second field-limiting mechanism has been proposed by Gomer (1979) who calculates that the ion-emission process is space-charge limited from the switch-on current onwards. He calculates that for a tube emitter the available liquid flow is much greater than is consumed by the ion-beam. Although the

liquid flow-rate will be considerably smaller for the thin-film wetted-needle emitter, the space-charge effect is likely to strongly limit the change in current as a function of field. The increase in current due to the pulse will be much smaller than for the solid-emitter, and the acceleration of the (approximately constant) flux of ions by the varying voltage during the pulse will merely result in a spread in energy of the ions, as observed. Evidently, in the absence of space-charge effects, to increase the field significantly in the hope of increasing the average charge of the ions, the pulse must raise the field significantly during the time for one monolayer of the liquid emitter surface to evaporate. For a 10% increase in field, at a 100 μA flux, this implies a pulse of 600 V amplitude and a risetime of order 10 pS: it seems unlikely that such pulses can be achieved in practice.

μS pulses

The work on μS -pulsing the emitter extends the work of Thompson and Frewett, reported at the 1979 Field Emission Symposium, to shorter pulse lengths. Pulses 70 μS in length and 500 V - 4 KV in amplitude were generated using thyristor stacks as switches, and applied to the emitter through a 500 pF capacitor. The effect on the emitter was observed by monitoring the current on the collector ((2) in figure 1), measured across a $1\text{K}\Omega$ resistor. For small pulses and moderate standing voltages the current increased and remained approximately constant during the pulse, with a small decrease when the pulse ended; the current recovered to its initial value in a time of order 100 μS (figure 9a). For larger pulses the current during the pulse oscillated briskly (figure 9b) and the decrease in current at the end of the pulse was more marked. For larger pulses still it was observed that the source current dropped

to zero at the end of the pulse (figure 9c) and only restarted after a time of ~ 2.6 mS, with a characteristic overshoot before settling to the DC level. It was also found to be possible to run the source with a standing voltage too low for steady-state current flow; the current then started when the pulse was applied (figure 9d). This type of operation seemed to be quite stable, at least over a period of thirty minutes, and might well have useful applications in the ion-beam lithography field.

References

1. A. J. Dixon: J. Phys. D, Appl. Phys 12 L77 1979
2. R. Gomer: Appl. Phys. 19 365 1979
3. S. V. Krishnaswamy and E. W. Mueller: Rev. Sci. Instr. 41 1409 1974
4. P. Sudreau, C. Colliex and J. Van de Walle: J. Physique - Lettres,
to be published.

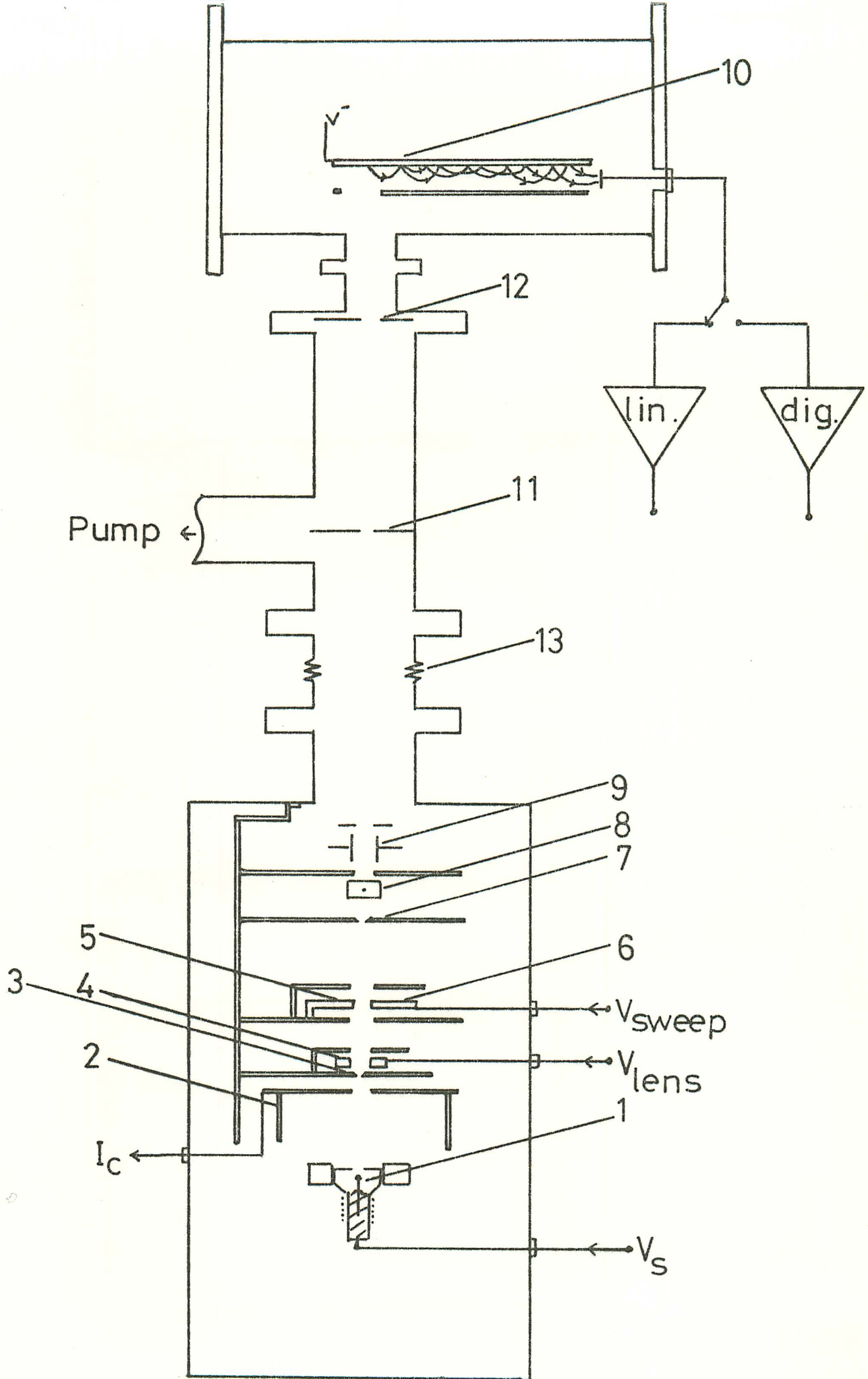


Figure 1.

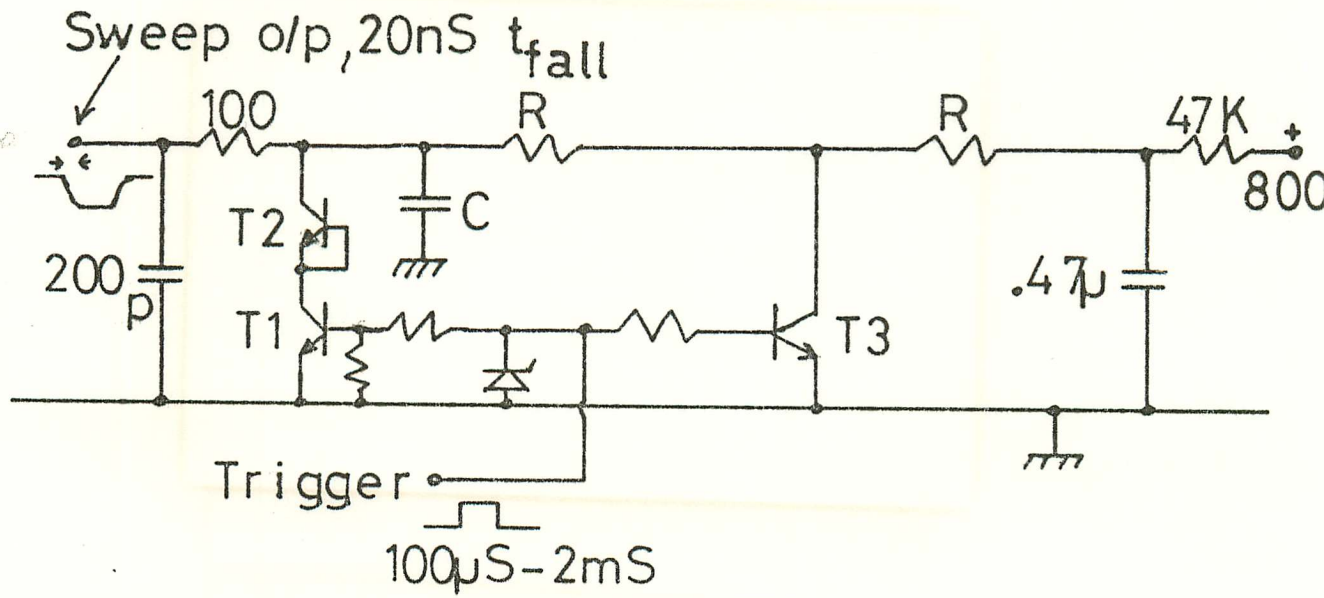


Figure 2.

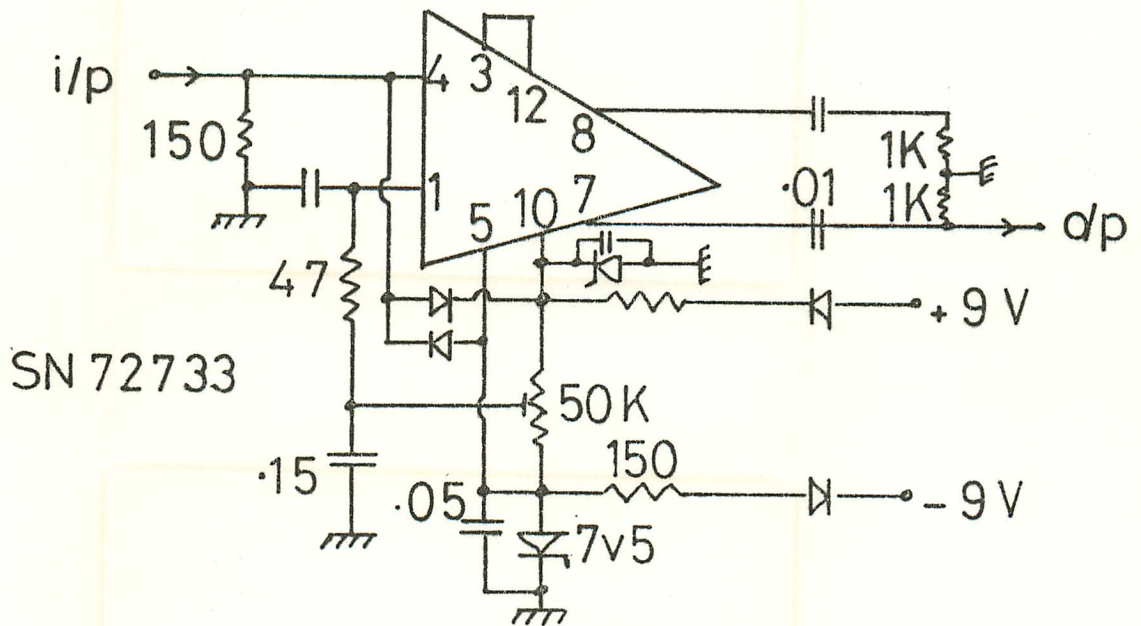
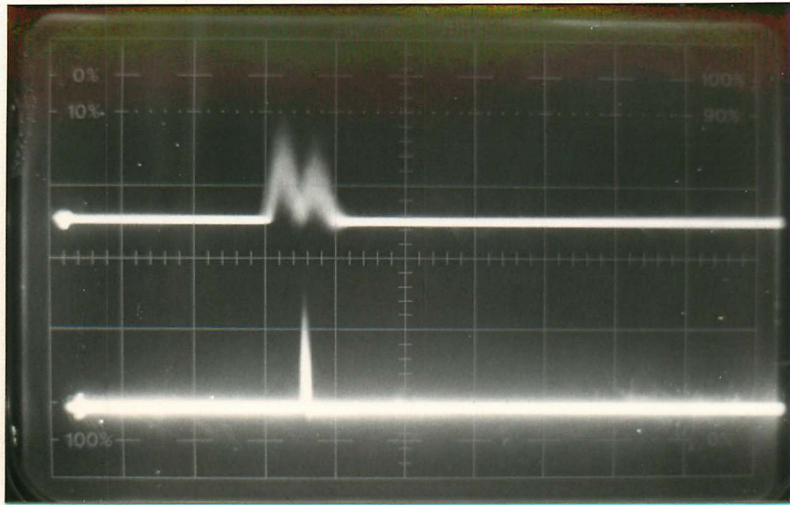
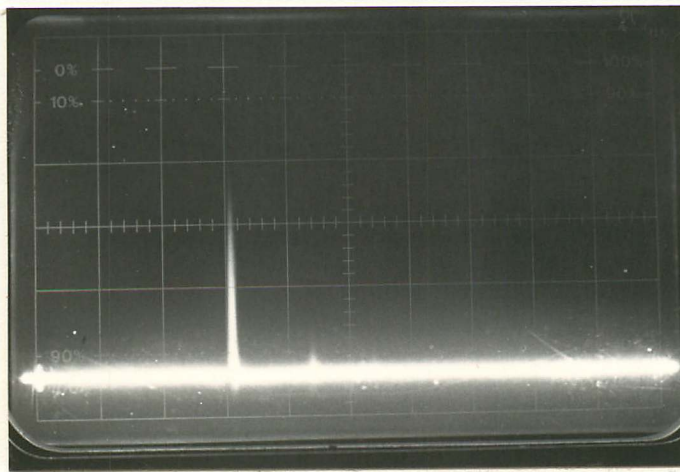


Figure 3.

a)



b)



c)

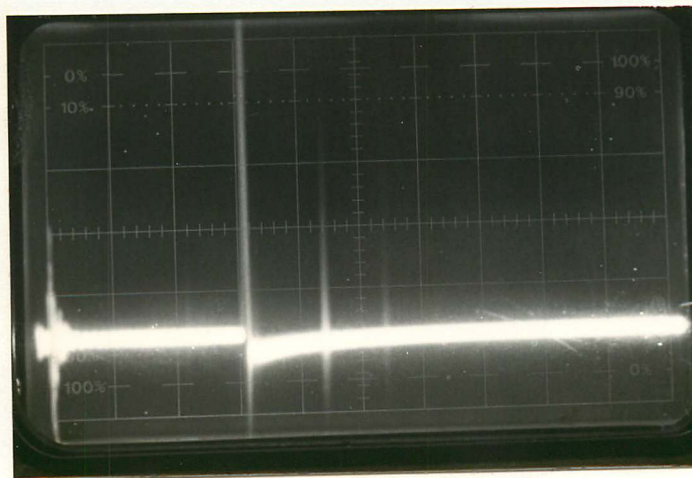
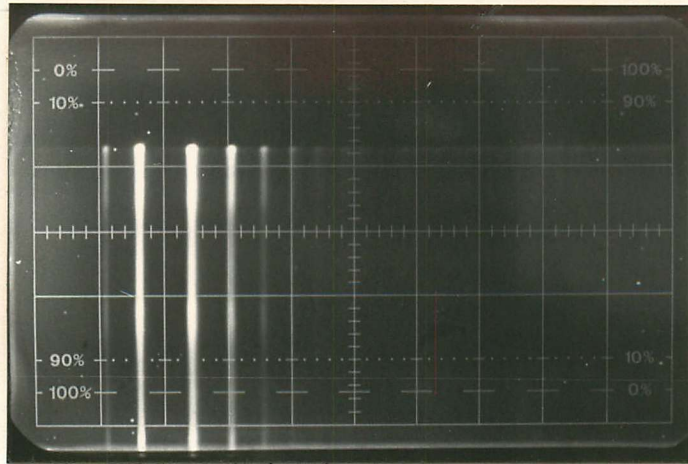


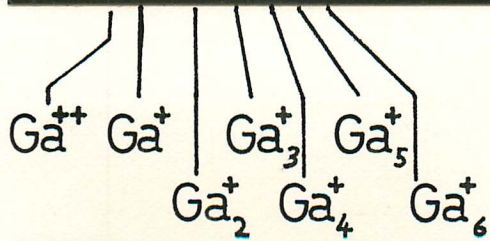
Figure 4. Output from the linear amplifier:-

- a) expanded trace showing resolved isotopes; b) showing Ga_2^+
c) $\times 10$, showing Ga^+ : $\sim 5-10\%$ Ga_2^+ : $\sim 2-4\%$ Ga_3^+ : $\sim \frac{1}{2}\%$ Ga^{++}

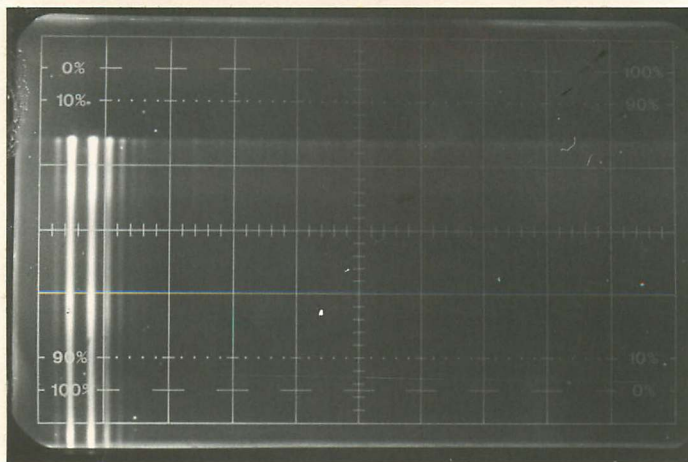
a.)



5 μ S/cm



b.)



10 μ S/cm

Figure 5; Output from the digital amplifier; oscilloscope photographs integrated over $\sim 10^4$ spectrometer sweeps, showing presence of Ga_n^+ clusters.

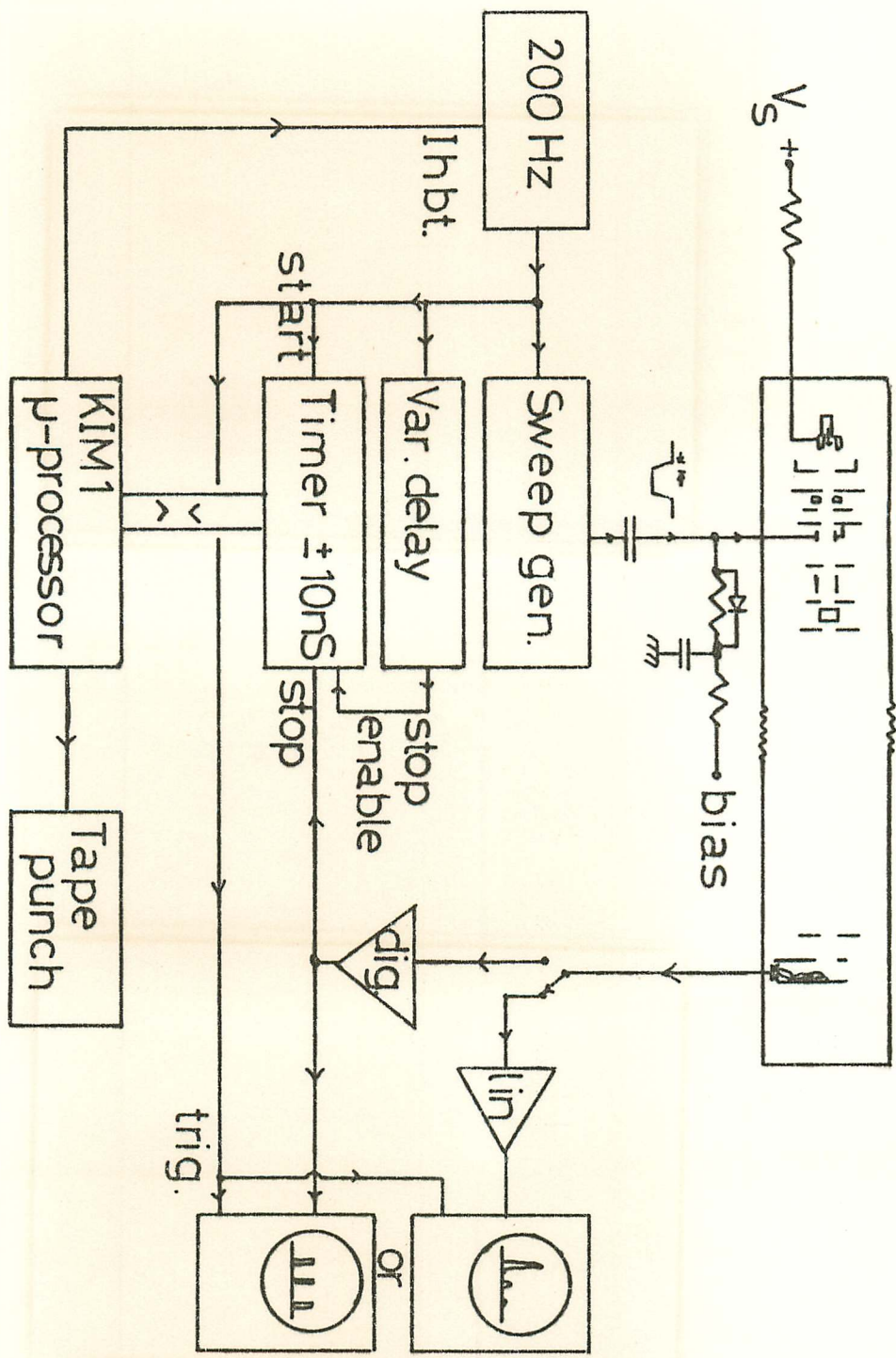


Figure 6.

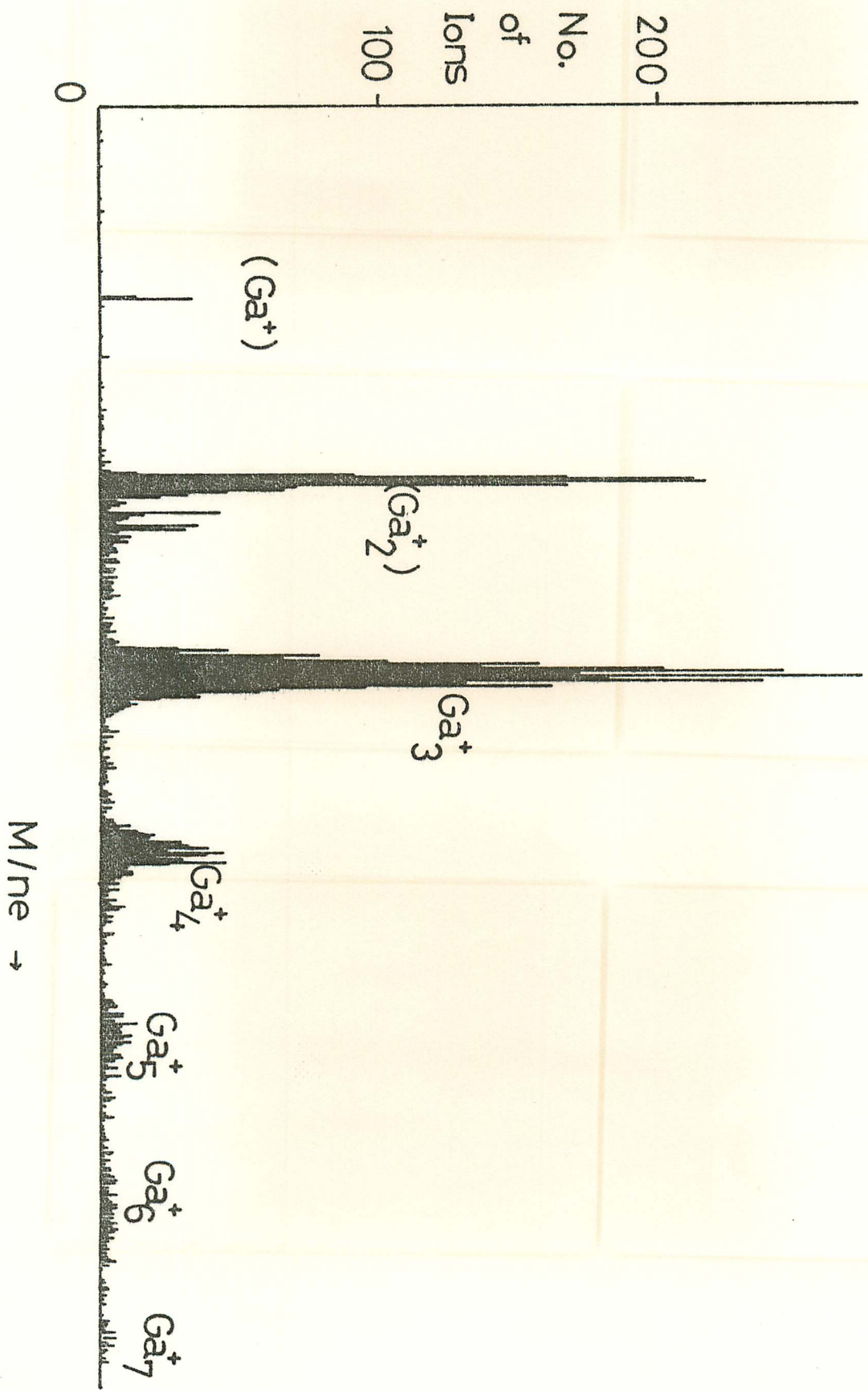
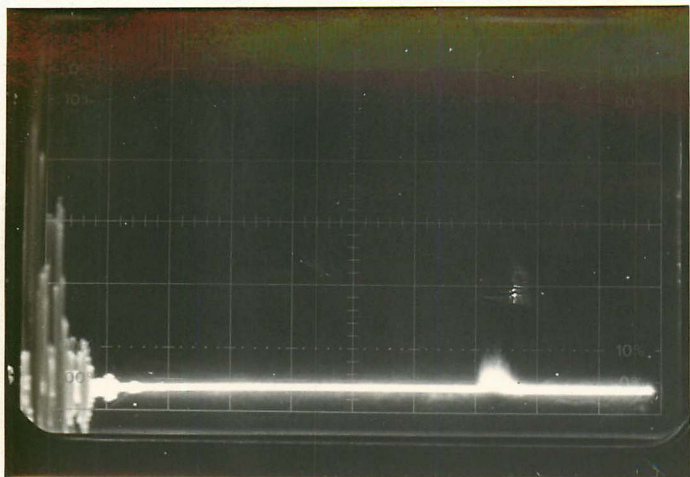
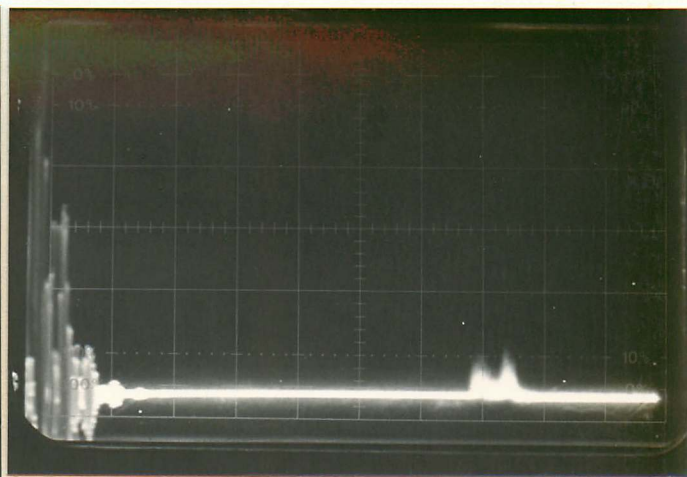


Figure 7.

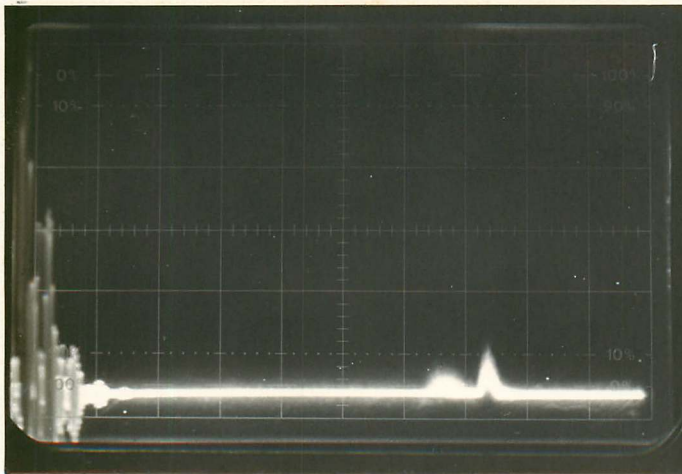
a)



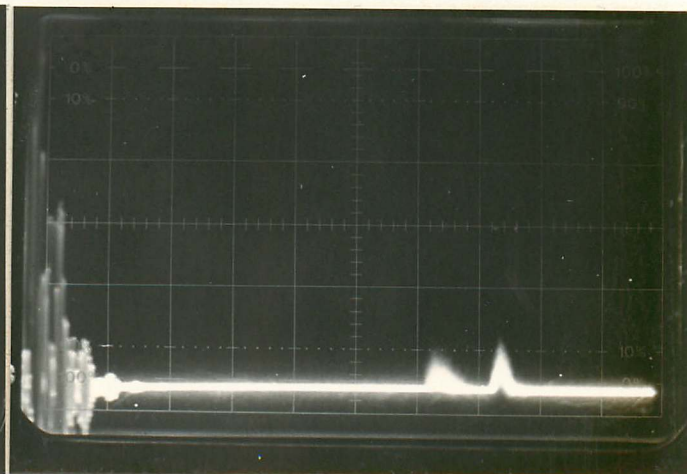
b)



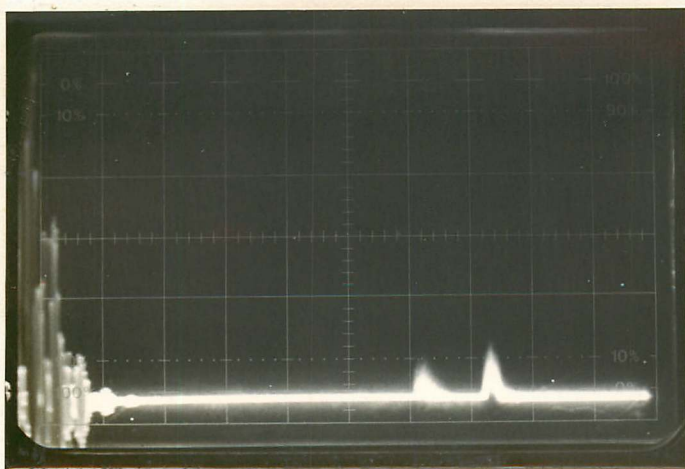
c)



d)



e)



f)

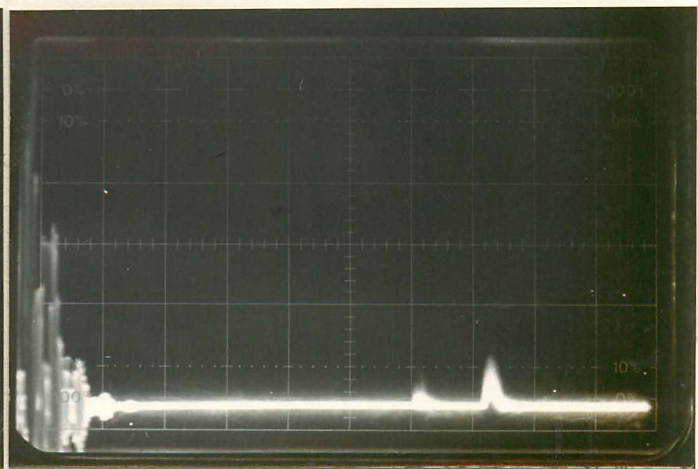
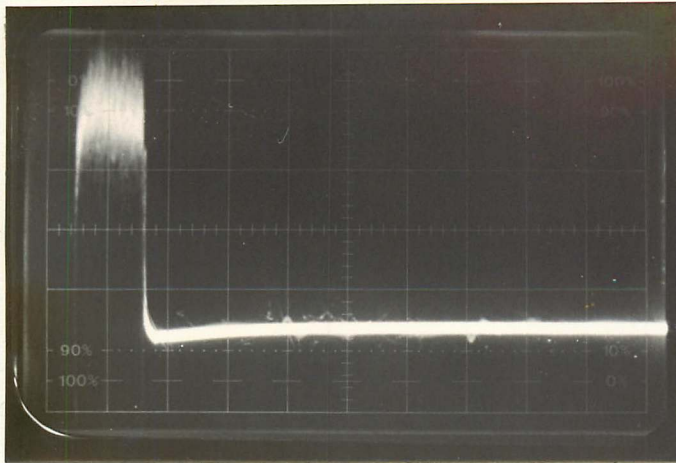
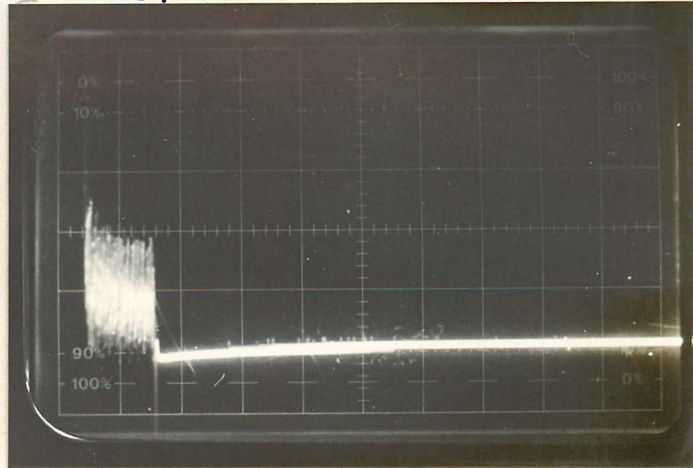


Figure 8, a-f in order of decreasing delay between pulse on Ga source and spectrometer start pulse; second peak due to high-energy Ga^+ .

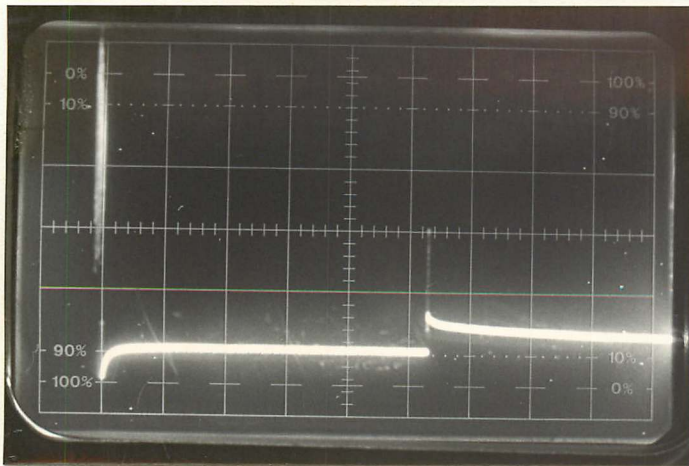
a) $50\mu\text{S/cm}$ $6+3\text{KV}$



b) $50\mu\text{S/cm}$ $6.24+3\text{KV}$



c) 0.5mS/cm $4.75+1\text{KV}$



d) $50\mu\text{S/cm}$ $4.7+2\text{KV}$

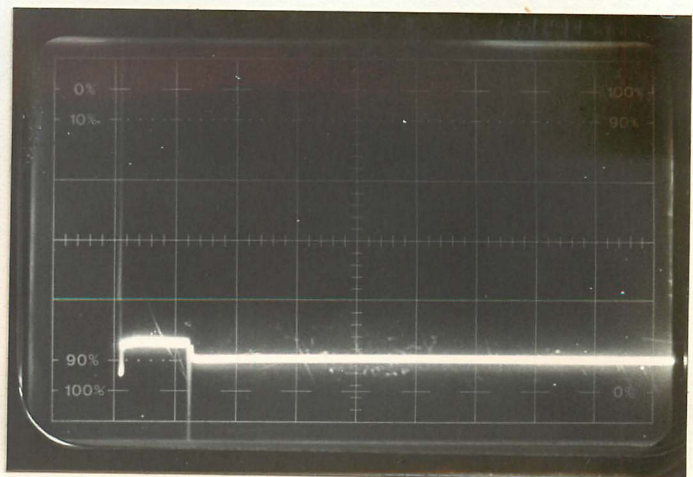


Figure 9; effect of 70 uS pulses on the current from the Ga emitter.